ACS OMEGA

http://pubs.acs.org/journal/acsodf

Article

Influence of Ions and pH on the Formation of Solid- and Liquid-like Melanin

Yi-chieh Chen,* Thomas Kendall, Philip Yip, Alastair Davy, Jan Sefcik, and Jens U. Sutter

Cite This: *ACS Omega* 2020, 5, 25059−25068

Read Online

ACCESS | Metrics & More | Article Recommendations

ABSTRACT: Melanin is a natural pigment with broadband absorption and effective ability to dissipate the energy absorbed. The macromolecular structure of melanin shows a delicate balance between short-range ordered and disordered structures without being a random aggregate. The presence of ions or the variation in pH or ionic strength can alter the self-assembly process which subsequently changes the structure of melanin. To understand these relationships, this study investigates the influence of ions and pH in melanin formation. The types of ions present and pH have a profound influence on the formation and structure of melanin particles, while only minor changes are observed in the absorption and excitation−emission analysis. In some conditions, the formation of discernible particles with significant refractive index contrast is avoided while retaining the spectroscopic characteristics of melanin, leading to liquid-like melanin. These findings identify potential pathways which can be used to manipulate the melanin macromolecular structure while providing the desired spectral properties to enable novel bio-engineering applications.

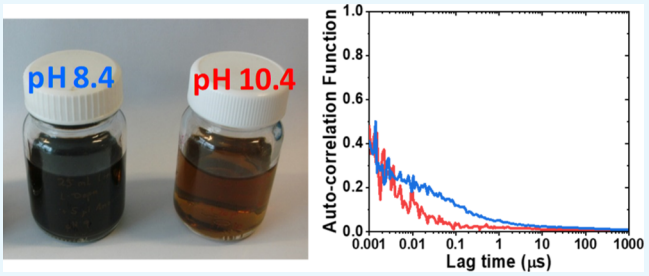

INTRODUCTION

Establishing a structure−function relationship has been one of the key aims of protein research,[1] and an important pathway to drug discovery.[2] While measurements of molecular constituents through spectroscopic methods or electrophoresis can reveal the function of a molecule or a protein under investigation,[3] characterizations through scattering techniques, fractionations, or imaging can provide structural information about the object.[4] Linking structure and function can then lead to a powerful breakthrough in the understanding of a molecule, a protein, or a cellular process.[5,6] Generating these links proves difficult when there are multiple inter-related functions or when the structure shows variations, as happens throughout living organisms.

Melanin comes with both these problems; it is a macromolecule well known for its broadband absorbance, and it usually forms various particles.[7,8] Melanin, typically synthesized by melanosomes, acts as a photo-protector to defend against UV radiation for many organisms, including animals, insects, plants, and fungi.[8,9] Melanin also exhibits myriad functions and plays a much more varied role.[10] For example, melanin is involved in the sequestration of ions.[11,12] It is also the main constituent of cephalopod ink for providing protection[13] and stabilizes the cell wall structure of fungi.[14] However, when it comes to the particle structure of melanin, a broad distribution of shapes and sizes have been reported.[7,8] Some of these variations could be because of the extraction and preparation techniques, but a puzzling variety remains. There is an ongoing quest to find the smallest possible entity that constitutes melanin; a fundamental unit or building block.[15,16]

Melanin exists in two primary forms—eumelanin, the typical black form of the molecule and the reddish-brown pheomelanin which forms with the presence of amino acid tyrosine to sustain the conversion of L-3,4-dihydroxy-L-phenylalanine (DOPA).[17] The presence of the L-cysteine and the tyrosinase sustains the reaction to form pheomelanin while a pure L-DOPA solution will generate only eumelanin. While the two tyrosinase-related proteins TRP1 and TRP2 help regulate the melanogenesis process, they are not necessary for the formation of pheomelanin.[18] The formation of melanin is governed by a wide range of parameters: temperature, pH, ionic strength, or small effector molecules. Excellent work has been done in revealing some of the initial reaction stages in the formation of eumelanin and pheomelanin.[7,16,19,20] Variation in the melanin structure can, in no small extent, be attributed to effectors in the cellular matrix. Changes in the pH have a strong influence on melanin formation[21] or disassembly.[22] When bio-engineering melanin at alkaline pH, some deviations in the structure from the biomimetic melanin might be

Received: April 28, 2020
Accepted: September 9, 2020
Published: September 23, 2020

https://dx.doi.org/10.1021/acsomega.0c01953
ACS Omega 2020, 5, 25059−25068

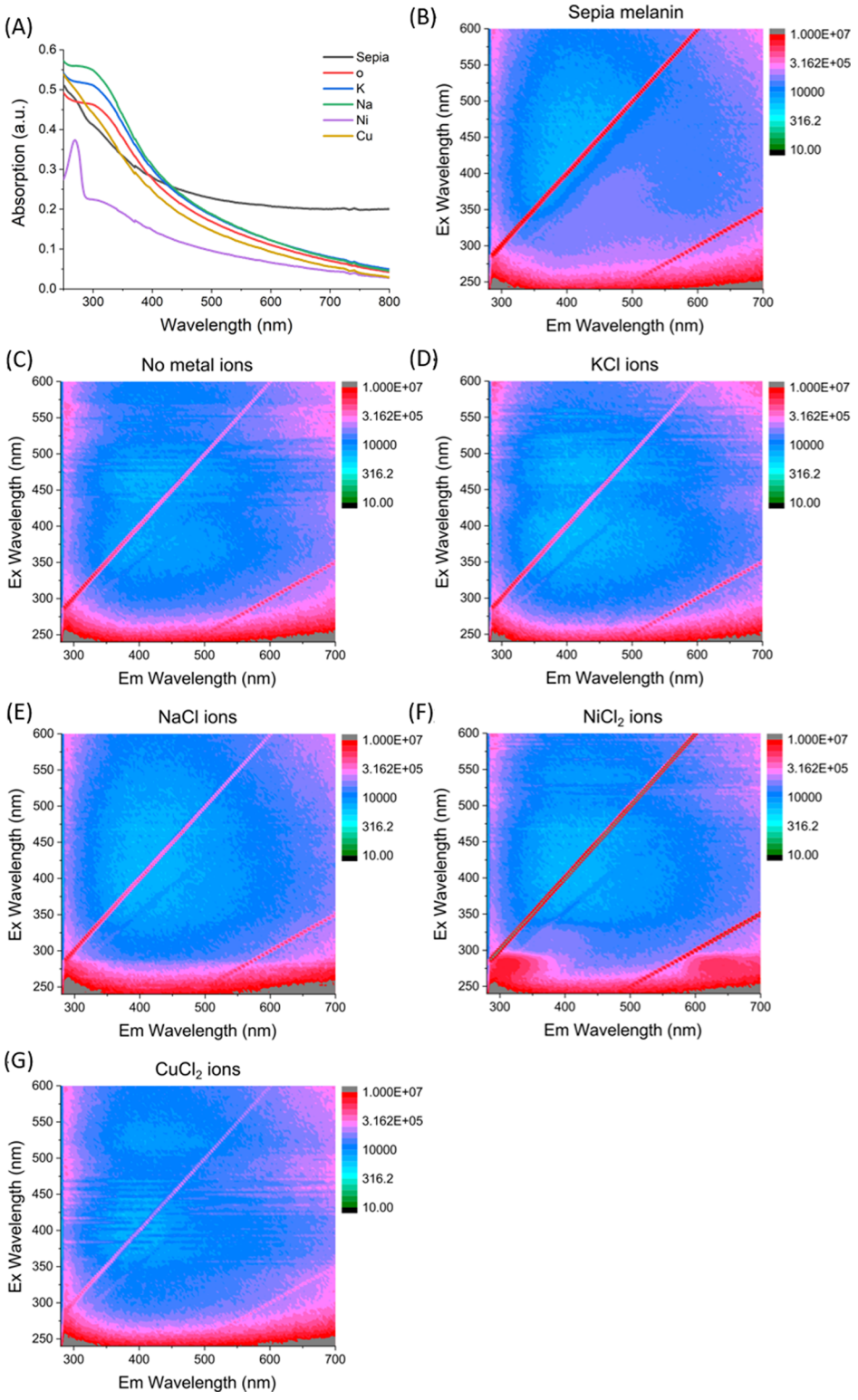

Figure 1. (A) Absorption spectra and (B–G) EEMs of melanin formed at pH 8.4 with different ions present. "o" in (A) denotes the absorption spectra for the melanin formed without the presence of ions. The Ex and Em on the axes correspond to the excitation and emission wavelength, respectively, in (B–G).

incurred.[23] The presence of physiological ions, potassium or sodium, does not influence the structure of melanin yet micronutrients such as copper or nickel do alter melanin's characteristics.[6,24] Micronutrients are essential elements required by organisms to orchestrate a range of physiological functions. Copper is involved in enabling proteins to perform essential metabolic functions and also required for the normal functioning of aerobic microorganisms, while nickel is known to be crucial on plant growth, the hydrolysis of urea, as well as nitrogen fixation.[25,26] Excellent work is available characterizing distinctive stages of eumelanin formation in detail.[27−30]

https://dx.doi.org/10.1021/acsomega.0c01953
ACS Omega 2020, 5, 25059−25068

There has been recent progress in linking measurements of functional characteristics to create multi-dimensional matrices of parameters.[31,32] For example, linking measurement of excitation and emission spectra yields a quantum yield map of melanin, also known as excitation−emission-matrix (EEM). An EEM contains a set of "spectral fingerprint" which is unique to melanin formed at a specific condition.[32] Here, we investigate the influence of physiological and micronutrient ions and pH on the formation of melanin. We use spectroscopic properties, namely, the absorption and EEM, of melanin to study the function of the macromolecule synthesized under the presence of various ions. Furthermore, dynamic light scattering (DLS) analysis is used to provide structure information about melanin synthesized under different ions and pH conditions. The technique collects optical density fluctuation caused by the structure of melanin to determine particle size. Combining the analysis from these techniques will gain novel insights into the structure−function relationship of melanin. In particular, we find that, while the spectroscopic function is retained for all ion and pH conditions investigated, we do not always find the particulate form of melanin.

EXPERIMENTAL METHODS

Materials. All chemicals were purchased from Sigma-Aldrich at the highest purities available. The lot numbers for chemicals that might show variation were: 3,4-dihydroxy-L-phenylalanine (D9628, Lot# SLBB4239V). *Sepia* melanin was purchased from Sigma-Aldrich [(CAS number 8049-97-6 (Lot 103H1023)] as suggested for standardization by d'Ischia et al.[28]

Synthesis of Melanin. Before synthesizing eumelanin, an L-DOPA stock solution of 1 mM was prepared by mixing L-DOPA with de-ionized water in a sonication bath for 10 min. The stock solution was then stored at 21 °C in the dark. Eumelanin was synthesized under aerial oxidation, following the standard laboratory melanogenesis protocols.[33] The nature pH of the solution is at 8.4, and ammonia was used to raise the pH to 10.7. For forming eumelanin at the presence of ions, metal ion aqueous stock solutions of 10 mM were added before aerial oxidation to a final concentration of 100 μM. $CuCl_2$, $NiCl_2$, NaCl, and KCl were used for providing physiological (K^+ and Na^+) and micronutrient (Cu^{2+} and Ni^{2+}) ions.

Sepia melanin solution was prepared by dissolving the powder in de-ionized water. The solution is then diluted to an optical density matching that of the 100 μM eumelanin formed without additional ions.

All synthesized melanin samples were left for five to ten days with regular absorbance measurements undertaken. Absorption was found to be stable after three days and remained so for weeks. Only fully reacted samples from L-DOPA were taken for the analysis presented here.

Absorption Spectroscopy. Collimated transmittance measurements were performed using a Jasco V-660 spectrophotometer. The melanin solutions were diluted by de-ionized water to a final concentration equivalent to 100 μM L-DOPA solution, and the obtained transmittance was converted to absorption spectra for further analysis. The dilution mitigates the potential interference of nonlinear multiple scattering effects caused by particles to alter the absorption obtained.[34] The same condition, as described in ref 35, was used for the acquisition.

Excitation−Emission Matrices. An EEM measurement produces a quantum yield map which links the emission characteristics using various excitation wavelengths.[31,32] This study used a Horiba Scientific Fluorolog 3−22 system with a 450 W xenon lamp for excitation and double grating excitation and emission monochromators. Excitation wavelengths from 240 to 600 nm were used, and the emitted fluorescence in the wavelengths of 280−700 nm was collected. Slits of the monochromators were set to 5 nm for both the excitation and emission pathway, and the integration time was 0.1 s. Measurement increments of 5 nm were set to reduce the total measurement time per sample without the loss of spectral detail. All EEMs were measured from the diluted samples (OD_{300} = 0.5) in a 6Q quartz cuvette. A background EEM from the blank water sample was collected in the same setup. To prevent possible precipitation, the samples were stirred during the measurement.

For processing the data, first, the signal from Rayleigh scattering was masked to allow clean subtraction of the background. This is followed by the procedure described by Riesz et al. to correct the inner-filter effects.[36] Each EEM intensity was multiplied by a scaling factor calculated from the absorption coefficient at both the excitation and emission wavelengths and subtracted by the background. All EEMs are shown in a logarithmic scale to present greater detail in regions of weak fluorescence.

Dynamic Light Scattering. The DLS measurements were performed using an ALV/LSE 5004 instrument with a laser wavelength of 632.8 nm. The intensity autocorrelation functions (ACFs) were obtained at a scattering angle of 90°, and the cumulant method was used to estimate the effective diffusion coefficient.[37] The mean hydrodynamic radius was then calculated using the Einstein−Stokes equation. The melanin samples were diluted by a ratio of 1:100 to a concentration equivalent to 10 μM L-DOPA using de-ionized water filtered by a 0.2 μm polyethersulfone syringe. Diluted melanin solutions were nearly colorless and fully transparent so that multiple scattering effects were minimal. Three replicates of the ACF for each sample were averaged, and the mean hydrodynamic radii of melanin particles were estimated.[37]

RESULTS AND DISCUSSION

Spectroscopic Properties of Melanin. *Sepia Melanin and Melanin Formed at pH 8.4.* While melanin seems to have more than one role in living systems, it is first and foremost a UV absorber. Figure 1A shows broadband absorption across the visible wavelength region for melanin formed at a natural pH environment (pH 8.4); the featureless characteristic of the spectra corresponds to melanin's dark appearance. The formation of melanin from the L-DOPA was traced by absorption spectroscopy in the wavelength region of 250−800 nm, and only the spectra of the fully reacted melanin samples are reported here. *Sepia* melanin exhibits a more balanced absorption intensity across the broad wavelength range investigated, while melanin formed from L-DOPA reveals a rapid decrease in absorption with the increase of wavelength. The presence of K^+ or Na^+ during melanin formation only results in small changes in the absorption intensity, compared to the spectrum for melanin formed without the presence of ions. All three spectra exhibit a broad and weak peak at around 320 nm. The presence of micronutrients, on the other hand, causes noticeable changes in the absorption spectra by either

https://dx.doi.org/10.1021/acsomega.0c01953
ACS Omega 2020, 5, 25059−25068

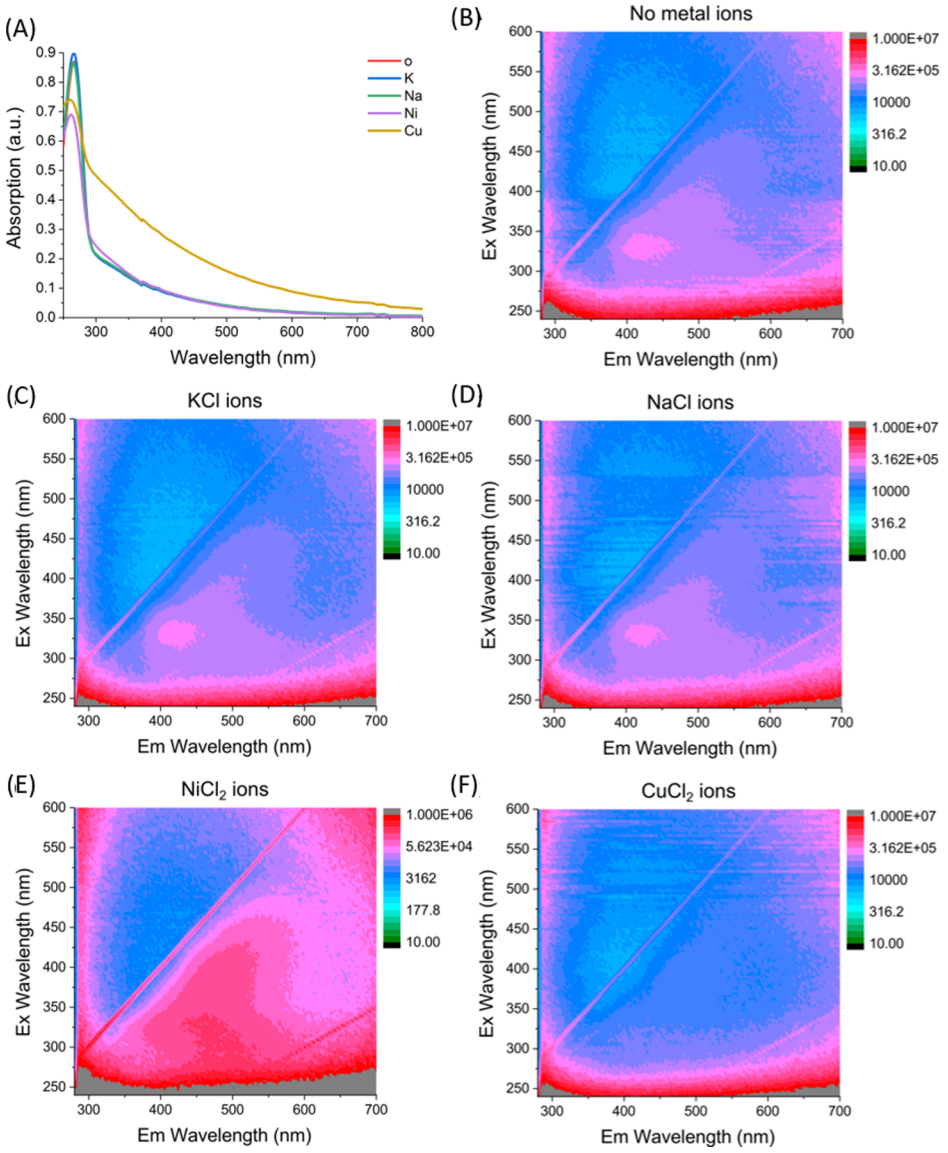

Figure 2. (A) Absorption spectra and (B–F) EEMs of melanin formed at pH 10.7 with different ions present. The Ex and Em wavelength from the axes correspond to the excitation and emission wavelength, respectively.

exhibiting an additional peak at 270 nm (in the case of Ni^{2+}) or the absence of the peaks at 320 nm (in the case of Cu^{2+}).

There are many theories developed to interpret the absorption characteristics of melanin and to relate them to the structure of melanin. The "chemical disorder" model of melanin assumes that the featureless broadband absorbance is achieved by chemical variations of melanin building blocks adding up to a total spectrum.[38] Different absorption peaks are suggested by the density functional theory, which calculates the highest occupied molecular orbital and the lowest unoccupied molecular orbital (HOMO–LUMO) energy gap of the redox states of melanin's fundamental building blocks, dihydroxyindole (DHI), and dihydroxyindole-2-carboxylic acid (DHICA).[39] Furthermore, the sheet structure of melanin can have a significant degree of variation by altering the ratio of DHI and DHICA and their different redox forms,[6] as DHICA generates an atypical form of melanin.[15,40] The number of indole molecules involved in the sheet structure might affect the absorption characteristics, as reported in the previous studies.[6,15,41] Assuming that the structure of melanin stabilizes the different redox states, the overall broadband absorption characteristics of melanin may constitute absorption characteristics of semiquinone, hydroquinone, and indolequinone states of DHI and DHICA.

To assign contributions of DHI and DHICA at each state using the absorption spectra, one needs to consider the structures associated with these building blocks and their optical characteristics. We previously observed the temporal evolution of the absorption spectrum, where gradual flattening of the absorption characteristics of the indole structures occurs as melanin forms.[32] The smooth and featureless absorption spectra, as shown in Figure 1A indicate no "missing element" or imbalance in the building blocks of melanin.

On the other hand, Figure 1B–G shows several interesting spectral features in the EEMs of natural melanin and melanin formed under different ion conditions at pH 8.4. A prominent fluorescence emission over a broad wavelength range in 280–700 nm can be observed from all samples when excited by a wavelength around 250 nm. All melanin formed at pH 8.4 exhibit exceptionally strong Rayleigh scattering, as suggested

https://dx.doi.org/10.1021/acsomega.0c01953
ACS Omega 2020, 5, 25059–25068

by the clearly resolved emission intensity from the nearby wavelength of the two diagonal lines in the EEMs. These two lines correspond to the first- and second-order Rayleigh scattering, which can be related to the elastic scattering of excitation light by particulates in the sample.[42,43] These lines usually are removed by either built-in software functions of the equipment or EEM data processing routine as they tend to mask and obstruct features in the measured EEM signal. In this study, the Rayleigh lines were retained to indicate elastic light scattering behavior of melanin.

Figure 1 also reveals distinctive excitation−emission areas which are specific to the ion conditions or the synthesis method. *Sepia* melanin exhibits more prominent first- and second-order Rayleigh lines, indicating the higher scattering capability of this natural melanin than that for the lab-synthesized melanin. The *Sepia* melanin also shows a rich fluorescence emission area in the wavelength region of 400−530 nm when excited at 300−400 nm. This feature is absent from all melanin generated from L-DOPA; the lab-synthesized melanin shows a featureless emission across a broad excitation−emission area. At pH 8.4, the presence of ions or the difference in synthesizing melanin does not change the EEMs significantly; similar EEMs are obtained for the lab-synthesized melanin. The observation is consistent with a previous study on L-DOPA-derived eumelanin fluorescence without or with K^+, Na^+, or Cu^{2+} ions.[35] The only exception for melanin formed at the natural pH environment is the EEM from melanin formed with Ni^{2+} support. Figure 1F exhibits an interesting broad red-purple excitation−emission area with exceptional strong intensity 300−350 nm when excited by a wavelength around 275 nm. The pronounced excitation−emission region observed from Ni^{2+}-supported melanin agrees with the absorption peak observed in Figure 1A for this melanin type.

Melanin Formed at pH 10.7. Increasing the pH toward more alkaline conditions can be used to speed up the formation process of melanin from L-DOPA. Figure 2A shows that all melanin formed at pH 10.7 exhibit a prominent peak around 265 nm. Most of the melanin formed at the higher pH exhibit a suppressed absorption outside the UV/near-UV wavelength region. Nearly identical spectra were observed for melanin formed at the presence of K^+ or Na^+; this could suggest that the formation process is less sensitive to such ion environments than those formed in the natural pH environment. However, the involvement of the micronutrients (Ni^{2+} and Cu^{2+}) in melanin formation results in a different response in the absorption property. Melanin formed with the Ni^{2+} support follows the overall absorption feature as those formed with K^+ or Na^+ support, and only exhibits a weak absorption peak at 265 nm. On the contrary, the Cu^{2+}-supported melanin exhibit a similar absorption spectrum in both pH conditions, suggesting that the effect of the pH on melanin formation might be relatively small at the present of this type of ion.

While one might assign the strong absorption peak at around 265 nm to the "unused" L-DOPA, the peak position does differ from the prominent L-DOPA absorption peak observed before forming melanin, and also vary slightly with different ion conditions used. Given the alkaline environment of the samples, it is possible to assign the peak for dopaquinone. The measurements by Robinson and Smyth identify L-DOPA with a peak at 285 nm and dopaquinone at 272 nm.[44] In this study, an absorption peak was identified at 280 nm for L-DOPA in the same solvent before forming melanin. Considering absorption measurement has a systematic drift of the peak position, this would place the dopaquinone peak at 267 nm, which would be consistent with the peaks shown in Figure 2A. While it is not possible to definitively identify the compound giving the 265 nm peak, given the high pH of the sample and the narrow nature of the peak, it is likely to correspond to a distinct single molecule in the quinone or semiquinone form.

Figures 1A and 2A suggest that the absorber function of the melanin macromolecule synthesized from the L-DOPA molecule is comparable to those reported in the previous study for the melanin fully reacted from L-DOPA.[27,33,45] Changes in the ion environment for forming melanin introduce slight alterations to the absorption characteristics. Assigning the peak at 265 nm to dopaquinone explains the lower absorption profile in the vis−NIR spectral region, as the system is not able to continue melanogenesis past dopaquinone. This results in a small subset of the starting L-DOPA molecule which can make it through to the DHI and DHICA stages. Only the spectra with Cu^{2+} resemble the profile at pH 8.4; it would suggest that copper allows more of the starting DOPA compound to react past the hydroquinone stage and continue down the melanogenesis pathway.

Similar to Figure 1A, Figure 2B−F show the EEMs for melanin samples corresponding to the sample conditions in Figure 2A. Several striking differences are observed when compared to the EEMs in Figure 1. First, the Rayleigh lines in the EEMs are much weaker for the melanin generated at pH 10.7, suggesting that the structure of the macromolecule has a far less light scattering property. The addition of Na^+ or K^+ ions does not significantly alter the EEM profile. The EEMs for melanin generated at this pH without any ion or with the presence of physiological ions (K^+ or Na^+) show similar characteristic to natural *Sepia* melanin at pH 8.4; the findings here further diminishes the importance of physiological ions on melanogenesis. The EEMs, as shown in Figure 2B−D, exhibit a broad excitation−emission area at 400−530 nm when excited at 300−400 nm, with a peak centered at 325 nm excitation and 425 nm emission. The change is likely due to the alterations related to the quinone ring fission.[23]

Interestingly, the involvement of the micronutrients in the melanin formation results in distinctive EEM responses, depending on the type of ions involved. In Figure 2E, the melanin formed in the presence of Ni^{2+} exhibits an excitation−emission area over a broad range of excitation (275−475 nm) and emission (350−650 nm) wavelength. The EEM profile for the Ni^{2+}-supported melanin is similar to those for the natural *Sepia* melanin, as shown in Figure 1B, but with stronger fluorescence. Unlike the cases at pH 8.4, the EEM profile of the Ni^{2+}-supported melanin is distinctive from the other melanin formed at higher pH, which suggests a significant change of this melanin. On the other hand, the EEMs for the Cu^{2+}-supported melanin resembles the lower pH samples without ions or with K^+ and Na^+, and the emission at 425 nm with 325 nm excitation is noticeably absent. The EEMs for the melanin formed in the presence of Cu^{2+} remains largely unaffected by the pH, as also suggested in the comparison of the corresponding absorption spectra. Because of the larger difference between the excitation and emission wavelengths, the distinctive EEM response of the Ni^{2+}-supported melanin does not manifest on the corresponding absorption spectrum.

Combining the absorption and EEM analysis above reveals the limitations of the spectroscopic measurements to assess the

https://dx.doi.org/10.1021/acsomega.0c01953
ACS Omega 2020, 5, 25059−25068

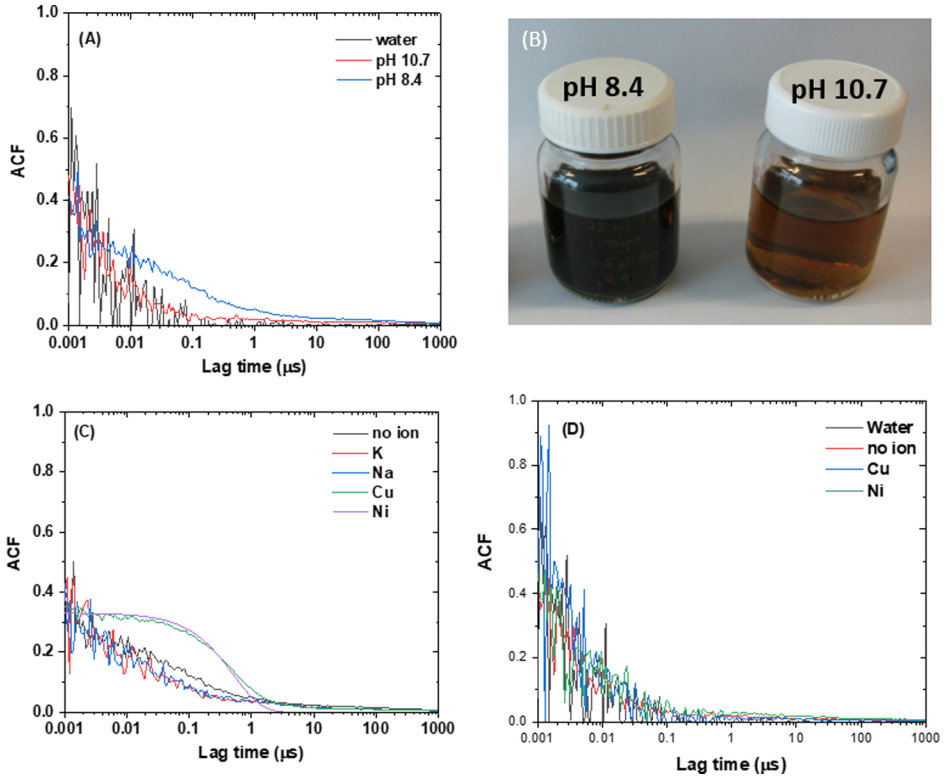

Figure 3. DLS ACFs. (A) ACF for pure water and diluted melanin generated from L-DOPA at pH 8.4 and 10.7 without the physiologically relevant ions. (B) Photos of undiluted melanin samples used to prepare a diluted solution in (A). (C,D) are melanin formed at pH 8.4 and pH 10.7, respectively, and under different ion conditions. The ACF for water is also included in (D) for comparison.

melanin structure further. While the absorption characteristics of the macromolecule is a critical feature of melanin, the information is not sufficient to understand the microscopic structure of the melanin or to establish the relationship between the function and structure of melanin. The metal ions studied here are known to only bind to specific functional groups which are available in multiple sites of the indole molecules including the hydroxyl, carboxylic, and amine groups.[46] For example, nickel ions can bind to the carboxyl and amine groups with the amine group being specific to L-DOPA and alter melanin structure by occupying the porphyrin ring.[47] However, different physiological ions present during the formation process only lead to relatively little variation in the overall absorbance, as shown in Figures 1A and 2A.

Copper ions show an affinity for all three functional groups available (hydroxyl, carboxyl, and amine) with hydroxyl and amine also being specific to L-DOPA. The presence of the Cu^{2+} in melanin formation is expected to strongly influence the size and forming of the initial oligomer sheets, and subsequently, alter the shape and size of possible protomolecules that stacked from these oligomer sheets.[29] This can be related to copper favoring a higher content of DHICA, which shifts in the balance between DHI and DHICA.[21] Because the carboxyl group of DHICA is favored as an edge-element around the forming sheets, altering the DHI to DHICA ratio by copper ions could lead to significant changes in the size and microscopic structure of melanin formed. However, the sheet formation as such does not contribute to the noticeable difference to melanin's broadband absorption. As the oligomerization of DHICA only causes a small redshift in the absorption spectrum,[48] it might "smooth out" the melanin spectrum without displaying structural-related characteristics. Considering the absorption characteristics observed, the analysis indicates the role of Cu^{2+} ions as a modulator in melanin formation.

On the other hand, excitation−emission matrices yield highly detailed spectroscopic characteristics of the fluorophore in melanin. The EEM results indicate that the presence of different ions and pH environment in the formation of melanin from L-DOPA has a distinct effect on the spectral characteristics of melanin. All EEMs exhibit characteristic areas of distinctive excitation−emission. In some cases, the difference in EEMs is relatively small, which seems to suggest the ions acting more as a modulator than changing melanin's optical characteristic. Although the radiative emission, as observed in Figures 1 and 2 can be considered as a "spectroscopic fingerprint" about the variation in the macromolecule,[49] melanin is a relatively weak fluorophore. A quantum yields of 3×10^{-3} for *Sepia* melanin and 6×10^{-4} for dopamine-derived eumelanin are reported.[38,50,51] Therefore, using melanin's fluorescence characteristics for understanding the melanin structure is typically hampered by its very low quantum yield. For achieving a thorough understanding, it is essential to link relevant measurements and findings from different analysis techniques.

Physical Properties of Melanin. While the EEMs and absorption spectra indicate that the presence and the type of ions at different pH can modulate the chemical/molecular properties of the melanin, these measurements are not sufficient to describe the self-assembled structure of melanin and the influence of modulation on the melanin structure. Furthermore, melanin particle sizes have been previously reported to range from 30 nm into several hundred nm,[8] and the size determined was strongly dependent on its source and

https://dx.doi.org/10.1021/acsomega.0c01953
ACS Omega 2020, 5, 25059−25068

method of extraction (for natural melanin) and its chemical genesis (for laboratory melanin). While the strong Rayleigh scattering observed in all EEMs, as show in Figures 1 and 2 might be attributed to the scattering effect caused by the melanin particles, the size of the particles cannot be directly extracted from the EEM analysis. To gain further understanding of the relationships between the structure and function, the microscopic structure of melanin particles was investigated using DLS measurements. This technique measures ACFs, which allow us to estimate mean hydrodynamic radii of suspended colloidal-scale particles, based in their Brownian motion. In this case, we can determine the largest scale structural parameter of melanin, that is, the particle size.

Melanin as synthesized is difficult to directly examine with DLS because of its dark color which is because of strong absorption of visible light, severely limiting the intensity of scattered light that can detected in DLS measurements. Therefore, DLS measurements in this study were taken from diluted melanin samples of a concentration equivalent to 10 μM L-DOPA. Figures 1A and 2A indicate low absorbance for all melanin samples investigated at the DLS laser wavelength, 632.8 nm, despite the fact that the sample concentration for the absorption analysis is 10 times higher (equivalent to 100 μM L-DOPA) than those for the DLS analysis. Therefore, the influence of absorption on DLS measurement was considered to be negligible, as also suggested by the low absorption and nearly colorless and transparent sample reported previously.[45]

Figure 3A shows the ACFs of melanin formed at different pH without the presence of any ions. An ACF measured for pure water is also included for comparison to show a typical solvent background corresponding to a molecularly homogeneous (in terms of refractive index contrast) liquid phase. The ACF for melanin particles formed at pH 8.4 clearly shows a decay pattern typically for a polydisperse population of colloidal scale particles with a mean hydrodynamic radius of 20 nm (estimated by the cumulant method). However, an ACF feature similar to pure water is observed for melanin formed at pH 10.7. This is surprising, as particles larger than about 1 nm with a significant refractive index contrast (as expected for solid melanin particles suspended in water) would show a clear ACF decay over and above the solvent background because of optical density fluctuations caused by Brownian motion of particles. In addition, a noticeable difference can be observed in the color of undiluted melanin samples, as shown in Figure 3B, corresponding to the synthesis conditions, as shown in Figure 3A, indicating that absorption is lower at higher pH, although both samples were nearly colorless and fully transparent upon dilution for DLS measurements. Figure 3C further compares the ACFs for melanin samples formed at pH 8.4 in the presence of various ions. Melanin particles formed without ions or with the presence of K^+ or Na^+ show a similar ACF feature corresponding to a polydisperse population of particles with a mean hydrodynamic radius of 20 nm. However, melanin formed in the presence of Ni^{2+} or Cu^{2+} ions shows distinctive exponential-like ACF decays corresponding to monodisperse populations of colloidal scale particles. The mean hydrodynamic radii estimated for melanin formed in the presence of Ni^{2+} and Cu^{2+} ions were 70 and 100 nm, respectively.

The 20 nm L-DOPA-derived melanin particle radius observed at pH 8.4 agrees with the so-called type A melanin particles reported by Büngeler and co-workers.[16] The type A particles were suggested to grow from rod-shaped protoparticles of about 6 nm in length and can be combined into forming the larger type B particle with a radius around 100 nm.[29] Our observations indicate that 20 nm melanin particles remain stable over prolonged periods, up to months after synthesis, and the formation of these particles is not influenced by the presence of physiologically relevant ions, K^+ or Na^+. Both ions are present in the human body in relatively high intracellular concentrations, around 140−150 mmol/L for potassium and 5−10 mmol/L for sodium,[52,53] and so far no indications have been found to link either of them to melanin formation. It is worth remembering that the majority (65−75%) of the potassium in the body is in the muscle and that the concentrations of the sodium are much higher (135−145 mmol/L) outside the cell.[52,53] It is also the case that ATPase pumps sodium out of the cell and potassium into the cell to maintain consistent concentrations of the two. It may be for these reasons that melanogenesis does not appear to be affected by the presence of the physiological ions such as sodium or potassium.[54] Furthermore, great care is required in translating findings derived from synthetic melanins to full biological systems. In living organisms, the size and shape of melanin particles are governed by a range of different parameters. For example, size and shape of melanins in vertebrates is determined by the organelle in which the melanin is produced. The shape of the organelle will determine the shape of the melanosome.[30]

As we have seen, the presence of Ni^{2+} and Cu^{2+} ions lead to the formation of much larger, nearly monodisperse particles with mean hydrodynamic radii of 70 and 100 nm, respectively. The larger one of these appears to be consistent with the type B particles reported previously.[16] Because of the monodispersity of particles formed in the presence of Ni^{2+} and Cu^{2+} ions, it is unlikely that colloidal aggregation via irreversible clustering of smaller particles is responsible, even under diffusion-limited conditions, as it would not lead to a stable final size.[55,56] Instead, this indicates that the presence of Ni^{2+} and Cu^{2+} ions leads to a distinct self-assembly process providing a well-defined structure and size of final melanin particles.

Changing the pH yields a further intriguing effect: melanin formed at an alkaline pH of 10.7, regardless of the ion condition, shows featureless ACFs similar to the one for pure water, as can been seen in Figure 3D. This means that no discernible melanin particles, in terms of a significant refractive index contrast with the surrounding aqueous phase, were formed at this condition, despite showing the clear spectral characteristics of melanin in EEM and absorption analysis. All conditions result in a smooth absorbance spectrum across the wavelength range investigated, with a strong UV absorption. No gaps are present to suggest any missing building block, according to the chemical disorder model, nor are random peaks observed to indicate an imbalance between the contributing building blocks. The process which adjusts the ratio of different redox states seems largely unaffected by the change of the pH. However, the absence of any ACFs beyond the aqueous background suggests a previously unreported form of melanin—liquid-like melanin.

Compared to the Rayleigh scattering lines, all melanin, except Ni^{2+} containing melanin (Figure 2E), show a reduced Rayleigh scattering intensity at this pH condition. The fact that ACFs observed in DLS measurements were not distinct from the aqueous background suggest that, despite the presence of

https://dx.doi.org/10.1021/acsomega.0c01953
ACS Omega 2020, 5, 25059−25068

the spectral (absorption and fluorescence) characteristics of melanin, there are no optical density fluctuations. Thus, melanin is present homogeneously dispersed within the solution, rather than suspended in the form of well-defined colloidal scale particles, and the size of such a molecular material is less than 1 nm. The finding is also consistent with the reduction in the Rayleigh scattering intensity, although Rayleigh scattering would also be present from components of homogenous molecular solutions. If particles were not formed, then it is possible that the synthesis of melanin at higher pH results in either a diverse solution of indole molecules, as per the chemical disorder model, or a collection of small oligomers similar to the porphyrin-like tetramers.

The findings from different analysis techniques used in this study align well with previous work showing that the de-stacking of melanin sheets does not necessarily obliterate their absorptive properties.[22,27,57] The reduced absorbance in the visible wavelength range for melanin formed at pH 10.7 resembles the absorption spectra of the disassembled *Sepia* melanin in a basic pH environment.[22] Furthermore, the strong emission at around 325 and 425 nm excitation−emission region, as shown in Figure 2B, agrees with the increased emission at 400 nm when exciting the disassembled melanin at 315 nm.[22] In this study, the absence of discernible particles with radii above 1 nm in DLS measurements could be because of the combination of alkaline environment and presence of an excess of metal ions (concentrations of ion to LOPA = 10:1) suppressing the stacking of oligomer sheets. Because this suppression would take place during the early stages of the melanogenesis, melanin particle formation is prevented altogether. This is in contrast to the de-stacking approach, where broad distributions of the disassembled particles size were reported.[22] It could explain the stronger UV absorption, as shown in Figure 2A, lack of measurable particles in DLS, and the numerous emission pathways that result in the EEMs of Figure 3. We give the term "liquid-like melanin" to reflect the unique state of the synthesized sample, where, despite no presence of particle form, all absorption and emission characteristics for melanin are achievable with no "missing element" or imbalance in the building blocks of melanin.

Overall, these findings indicate potential challenges in distinguishing different melanin using the spectroscopic analysis alone. Simple changes in the melanin formation environment, such as pH and metal ions, could lead to significant alterations in the melanin structure, which could be challenging to identify from absorption or fluorescence measurements. However, a better understanding of different melanin self-assembly pathways can be achieved by investigating the structure of melanin. In this study, the identification of a new form of liquid-like melanin structure was achieved by combining the information obtained from spectroscopic analysis and DLS measurements. This study demonstrates how the link between structure and function established by using complementary characterization techniques can provide new insights into behavior of macromolecules. This will lead to a deeper understanding and open opportunities based on the utilization of liquid-like melanin or similar macromolecule for novel bio-engineering applications, such as the use of melanin nanocomposite or melanin-type films in optoelectronic devices, where the pliability of the melanin structure without compromising its functionality is desired.[58,59]

CONCLUSIONS

The findings in this study suggest a previously unreported form of liquid-like melanin synthesized at alkaline conditions. The observation of the liquid-like melanin is supported by other studies which suggest that the absorption properties of melanin may not require a particulate melanin structure. Metal ions can be an important effector to melanin formation. Micronutrient ions, such as Ni^{2+} and Cu^{2+}, can significantly alter the emission pathway, particularly for melanin formed at higher pH. Physiological ions (K^+ and Na^+) only acts as a modulator in changing the absorption and emission characteristics. The effect of pH results in the most intriguing change. It leads to no discernible particle form for melanin formed at alkaline conditions, regardless of the ion conditions in the melanin synthesis, and the formation of distinctive melanin particle types under neutral pH and various ion conditions. The study demonstrates an approach to manipulate the melanin macromolecular structure and a means of utilizing and linking the functional and structural analysis to understand questions about the structure−function relation of melanin.

AUTHOR INFORMATION

Corresponding Author

Yi-chieh Chen − *Department of Chemical and Process Engineering, University of Strathclyde, Glasgow G1 1XJ, U.K.*; orcid.org/0000-0002-8307-0666; Email: yichieh.chen@strath.ac.uk

Authors

Thomas Kendall − *Department of Chemical and Process Engineering, University of Strathclyde, Glasgow G1 1XJ, U.K.*

Philip Yip − *Horiba IBH Ltd., Glasgow G3 8HB, Scotland, U.K.; Photophysics Group, Centre for Molecular Nanometrology, Department of Physics, The Scottish Universities Physics Alliance, University of Strathclyde, Glasgow G4 0NG, U.K.*

Alastair Davy − *Photophysics Group, Centre for Molecular Nanometrology, Department of Physics, The Scottish Universities Physics Alliance, University of Strathclyde, Glasgow G4 0NG, U.K.*

Jan Sefcik − *Department of Chemical and Process Engineering, University of Strathclyde, Glasgow G1 1XJ, U.K.*

Jens U. Sutter − *Photophysics Group, Centre for Molecular Nanometrology, Department of Physics, The Scottish Universities Physics Alliance, University of Strathclyde, Glasgow G4 0NG, U.K.*

Complete contact information is available at: https://pubs.acs.org/10.1021/acsomega.0c01953

Author Contributions

The manuscript was written through the contributions of all the authors. All the authors have given approval to the final version of the manuscript.

Notes

The authors declare no competing financial interest.

ACKNOWLEDGMENTS

Alastair Davy is grateful for support from the EPSRC and MRC Centre for Doctoral Training in Optical and Medical Imaging (OPTIMA, Grant Ref: EP/L016559/1) Thomas Kendall and Jan Sefcik are grateful for support from EPSRC and the Doctoral Training Centre in Continuous Manufactur-

ing and Crystallisation (Grant Ref: EP/K503289/1) and Centre for Innovative Manufacturing in Continuous Manufacturing and Crystallisation (Grant Ref: EP/I033459/1).

■ ABBREVIATIONS

ACF, autocorrelation function; ATPase, adenylpyrophosphatase; DHI, dihydroxyindole; DHICA, dihydroxyindole-2-carboxylic acid; DOPA, 3,4-dihydroxy-L-phenylalanine; DLS, dynamic light scattering; EEM, excitation−emission matrix; HOMO−LUMO, highest-occupied molecular-orbital to lowest-unoccupied-molecular-orbital; NIR, near infra-red; UV, ultra-violet

■ REFERENCES

(1) Reis, R.; Moraes, I. Structural biology and structure−function relationships of membrane proteins. *Biochem. Soc. Trans.* **2019**, *47*, 47−61.
(2) Nair, P. C.; Miners, J. O. Molecular dynamics simulations: from structure function relationships to drug discovery. *Silico Pharmacol.* **2014**, *2*, 4.
(3) Raman, N. M.; Ramasamy, S. Genetic validation and spectroscopic detailing of DHN-melanin extracted from an environmental fungus. *Biochem. Biophys. Rep* **2017**, *12*, 98−107.
(4) Xin, C.; Ma, J.-H.; Tan, C.-J.; Yang, Z.; Ye, F.; Long, C.; Ye, S.; Hou, D.-B. Preparation of melanin from Catharsius molossus L. and preliminary study on its chemical structure. *J. Biosci. Bioeng.* **2015**, *119*, 446−454.
(5) Alfieri, M. L.; Micillo, R.; Panzella, L.; Crescenzi, O.; Oscurato, S. L.; Maddalena, P.; Napolitano, A.; Ball, V.; d'Ischia, M. Structural Basis of Polydopamine Film Formation: Probing 5,6-Dihydroxyindole-Based Eumelanin Type Units and the Porphyrin Issue. *ACS Appl. Mater. Interfaces* **2018**, *10*, 7670−7680.
(6) Kaxiras, E.; Tsolakidis, A.; Zonios, G.; Meng, S. Structural Model of Eumelanin. *Phys. Rev. Lett.* **2006**, *97*, 218102.
(7) d'Ischia, M.; Wakamatsu, K.; Cicoira, F.; Di Mauro, E.; Garcia-Borron, J. C.; Commo, S.; Galván, I.; Ghanem, G.; Kenzo, K.; Meredith, P.; Pezzella, A.; Santato, C.; Sarna, T.; Simon, J. D.; Zecca, L.; Zucca, F. A.; Napolitano, A.; Ito, S. Melanins and melanogenesis: from pigment cells to human health and technological applications. *Pigm. Cell Melanoma Res.* **2015**, *28*, 520−544.
(8) Kollias, N.; Sayre, R. M.; Zeise, L.; Chedekel, M. R. New trends in photobiology: Photoprotection by melanin. *J. Photochem. Photobiol., B* **1991**, *9*, 135−160.
(9) Randhawa, M.; Seo, I.; Liebel, F.; Southall, M. D.; Kollias, N.; Ruvolo, E. Visible Light Induces Melanogenesis in Human Skin through a Photoadaptive Response. *PLoS One* **2015**, *10*, No. e0130949.
(10) Xie, W.; Pakdel, E.; Liang, Y.; Kim, Y. J.; Liu, D.; Sun, L.; Wang, X. Natural Eumelanin and Its Derivatives as Multifunctional Materials for Bioinspired Applications: A Review. *Biomacromolecules* **2019**, *20*, 4312−4331.
(11) Fogarty, R. V.; Tobin, J. M. Fungal melanins and their interactions with metals. *Enzyme Microb. Technol.* **1996**, *19*, 311−317.
(12) Enochs, W. S.; Sarna, T.; Zecca, L.; Riley, P. A.; Swartz, H. M. The roles of neuromelanin, binding of metal ions, and oxidative cytotoxicity in the pathogenesis of Parkinson's disease: A hypothesis. *J. Neural Transm.* **1994**, *7*, 83−100.
(13) Palumbo, A.; Poli, A.; Di Cosmo, A.; d'Ischia, M. N-Methyl-d-aspartate Receptor Stimulation Activates Tyrosinase and Promotes Melanin Synthesis in the Ink Gland of the Cuttlefish Sepia officinalis through the Nitric Oxide/cGMP Signal Transduction Pathway: A Novel Possible Role for Glutamate as Physiologic Activator of Melanogenesis. *J. Biol. Chem.* **2000**, *275*, 16885−16890.
(14) Eisenman, H. C.; Casadevall, A. Synthesis and assembly of fungal melanin. *Appl. Microbiol. Biotechnol.* **2012**, *93*, 931−940.
(15) Meng, S.; Kaxiras, E. Theoretical Models of Eumelanin Protomolecules and their Optical Properties. *Biophys. J.* **2008**, *94*, 2095−2105.
(16) Büngeler, A.; Hämisch, B.; Huber, K.; Bremser, W.; Strube, O. I. Insight into the Final Step of the Supramolecular Buildup of Eumelanin. *Langmuir* **2017**, *33*, 6895−6901.
(17) Ito, S. A Chemist's View of Melanogenesis. *Pigm. Cell Res.* **2003**, *16*, 230−236.
(18) del Marmol, V.; Ito, S.; Bouchard, B.; Libert, A.; Wakamatsu, K.; Ghanem, G.; Solano, F. Cysteine Deprivation Promotes Eumelanogenesis in Human Melanoma Cells. *J. Invest. Dermatol.* **1996**, *107*, 698−702.
(19) Prampolini, G.; Cacelli, I.; Ferretti, A. Intermolecular interactions in eumelanins: a computational bottom-up approach. I. small building blocks. *RSC Adv.* **2015**, *5*, 38513−38526.
(20) Micillo, R.; Panzella, L.; Koike, K.; Monfrecola, G.; Napolitano, A.; d'Ischia, M. "Fifty Shades" of Black and Red or How Carboxyl Groups Fine Tune Eumelanin and Pheomelanin Properties. *Int. J. Mol. Sci.* **2016**, *17*, 746.
(21) Ito, S.; Suzuki, N.; Takebayashi, S.; Commo, S.; Wakamatsu, K. Neutral pH and copper ions promote eumelanogenesis after the dopachrome stage. *Pigm. Cell Melanoma Res.* **2013**, *26*, 817−825.
(22) Ju, K.-Y.; Kang, J.; Chang, J. H.; Lee, J.-K. Clue to Understanding the Janus Behavior of Eumelanin: Investigating the Relationship between Hierarchical Assembly Structure of Eumelanin and Its Photophysical Properties. *Biomacromolecules* **2016**, *17*, 2860−2872.
(23) Prota, G. *Melanins and Melanogenesis*; Academic Press: San Diago, CA, USA, 1992.
(24) Birch, D. J. S.; Sutter, J. U. The effect of copper on eumelanin photophysics and morphology. *Imaging, Manipulation, and Analysis of Biomolecules, Cells, and Tissues XI*; SPIE BIOS: San Francisco, California, United States, 2013; p 858705.
(25) Yusuf, M.; Fariduddin, Q.; Hayat, S.; Ahmad, A. Nickel: An Overview of Uptake, Essentiality and Toxicity in Plants. *Bull. Environ. Contam. Toxicol.* **2011**, *86*, 1−17.
(26) Hänsch, R.; Mendel, R. R. Physiological functions of mineral micronutrients (Cu, Zn, Mn, Fe, Ni, Mo, B, Cl). *Curr. Opin. Plant Biol.* **2009**, *12*, 259−266.
(27) Watt, A. A. R.; Bothma, J. P.; Meredith, P. The supramolecular structure of melanin. *Soft Matter* **2009**, *5*, 3754−3760.
(28) d'Ischia, M.; Wakamatsu, K.; Napolitano, A.; Briganti, S.; Garcia-Borron, J.-C.; Kovacs, D.; Meredith, P.; Pezzella, A.; Picardo, M.; Sarna, T.; Simon, J. D.; Ito, S. Melanins and melanogenesis: methods, standards, protocols. *Pigm. Cell Melanoma Res.* **2013**, *26*, 616−633.
(29) Büngeler, A.; Hämisch, B.; Strube, O. The Supramolecular Buildup of Eumelanin: Structures, Mechanisms, Controllability. *Int. J. Mol. Sci.* **2017**, *18*, 1901.
(30) D'Alba, L.; Shawkey, M. D. Melanosomes: Biogenesis, Properties, and Evolution of an Ancient Organelle. *Physiol. Rev.* **2019**, *99*, 1−19.
(31) Nighswander-Rempel, S. P.; Riesz, J.; Gilmore, J.; Bothma, J. P.; Meredith, P. Quantitative Fluorescence Excitation Spectra of Synthetic Eumelanin. *J. Phys. Chem. B* **2005**, *109*, 20629−20635.
(32) Yip, P.; Sutter, J. U. Tracking the formation of eumelanin from L-Dopa using coupled measurements. *Methods Appl. Fluoresc.* **2018**, *6*, 027001.
(33) Della Vecchia, N. F.; Avolio, R.; Alfè, M.; Errico, M. E.; Napolitano, A.; d'Ischia, M. Building-Block Diversity in Polydopamine Underpins a Multifunctional Eumelanin-Type Platform Tunable Through a Quinone Control Point. *Adv. Funct. Mater.* **2013**, *23*, 1331−1340.
(34) Steponavicius, R.; Thennadil, S. N. Extraction of Chemical Information of Suspensions Using Radiative Transfer Theory to Remove Multiple Scattering Effects: Application to a Model Two-Component System. *Anal. Chem.* **2009**, *81*, 7713−7723.
(35) Sutter, J.-U.; Birch, D. J. S. Metal ion influence on eumelanin fluorescence and structure. *Methods Appl. Fluoresc.* **2014**, *2*, 024005.

https://dx.doi.org/10.1021/acsomega.0c01953
ACS Omega 2020, 5, 25059−25068

(36) Riesz, J.; Sarna, T.; Meredith, P. Radiative Relaxation in Synthetic Pheomelanin. *J. Phys. Chem. B* **2006**, *110*, 13985−13990.
(37) Sandkühler, P.; Sefcik, J.; Morbidelli, M. Scaling of the Kinetics of Slow Aggregation and Gel Formation for a Fluorinated Polymer Colloid. *Langmuir* **2005**, *21*, 2062−2077.
(38) Meredith, P.; Powell, B. J.; Riesz, J.; Nighswander-Rempel, S. P.; Pederson, M. R.; Moore, E. G. Towards structure−property−function relationships for eumelanin. *Soft Matter* **2006**, *2*, 37−44.
(39) Powell, B. J.; Baruah, T.; Bernstein, N.; Brake, K.; McKenzie, R. H.; Meredith, P.; Pederson, M. R. A first-principles density-functional calculation of the electronic and vibrational structure of the key melanin monomers. *J. Chem. Phys.* **2004**, *120*, 8608−8615.
(40) Panzella, L.; Gentile, G.; D'Errico, G.; Della Vecchia, N. F.; Errico, M. E.; Napolitano, A.; Carfagna, C.; d'Ischia, M. Atypical Structural and π-Electron Features of a Melanin Polymer That Lead to Superior Free-Radical-Scavenging Properties. *Angew. Chem., Int. Ed.* **2013**, *52*, 12684−12687.
(41) Chen, C.-T.; Chuang, C.; Cao, J.; Ball, V.; Ruch, D.; Buehler, M. J. Excitonic effects from geometric order and disorder explain broadband optical absorption in eumelanin. *Nat. Commun.* **2014**, *5*, 3859.
(42) Larsson, T.; Wedborg, M.; Turner, D. Correction of inner-filter effect in fluorescence excitation-emission matrix spectrometry using Raman scatter. *Anal. Chim. Acta* **2007**, *583*, 357−363.
(43) Lawaetz, A. J.; Stedmon, C. A. Fluorescence Intensity Calibration Using the Raman Scatter Peak of Water. *Appl. Spectrosc.* **2009**, *63*, 936−940.
(44) Robinson, G. M.; Smyth, M. R. Simultaneous Determination of Products and Intermediates of L-Dopa Oxidation Using Capillary Electrophoresis With Diode-array Detection. *Analyst* **1997**, *122*, 797−802.
(45) Ou-Yang, H.; Stamatas, G.; Kollias, N. Spectral Responses of Melanin to Ultraviolet A Irradiation. *J. Invest. Dermatol.* **2004**, *122*, 492−496.
(46) Di Mauro, E.; Xu, R.; Soliveri, G.; Santato, C. Natural melanin pigments and their interfaces with metal ions and oxides: emerging concepts and technologies. *MRS Commun.* **2017**, *7*, 141−151.
(47) Kim, Y. J.; Khetan, A.; Wu, W.; Chun, S.-E.; Viswanathan, V.; Whitacre, J. F.; Bettinger, C. J. Evidence of Porphyrin-Like Structures in Natural Melanin Pigments Using Electrochemical Fingerprinting. *Adv. Mater.* **2016**, *28*, 3173−3180.
(48) Ito, S.; Nicol, J. A. C. Isolation of oligomers of 5,6-dihydroxyindole-2-carboxylic acid from the eye of the catfish. *Biochem. J.* **1974**, *143*, 207−217.
(49) Gilmore, A. M. *How to Collect National Institute of Standards and Technology (NIST) Traceable Fluorescence Excitation and Emission Spectra*; Humana Press: Totowa, NJ, 2014; Vol. *1076*.
(50) Nofsinger, J. B.; Forest, S. E.; Simon, J. D. Explanation for the Disparity among Absorption and Action Spectra of Eumelanin. *J. Phys. Chem. B* **1999**, *103*, 11428−11432.
(51) Nofsinger, J. B.; Ye, T.; Simon, J. D. Ultrafast Nonradiative Relaxation Dynamics of Eumelanin. *J. Phys. Chem. B* **2001**, *105*, 2864−2866.
(52) Porth, C. *Essentials of Pathophysiology: Concepts of Altered Health States*; Lippincott Williams & Wilkins, 2011.
(53) Stoller, J. K.; Michota, F. A.; Mandell, B. F. *The Cleveland Clinic Foundation Intensive Review of Internal Medicine*; Lippincott William & Wilkins, 2009; Chapter 49.
(54) Ronco, C.; Bellomo, R.; Kellum, J. *Critical Care Nephrology*; Elsevier Health Sciences, 2009; Chapter 99.
(55) Wu, H.; Lattuada, M.; Sandkühler, P.; Sefcik, J.; Morbidelli, M. Role of Sedimentation and Buoyancy on the Kinetics of Diffusion Limited Colloidal Aggregation. *Langmuir* **2003**, *19*, 10710−10718.
(56) Lattuada, M.; Wu, H.; Sefcik, J.; Morbidelli, M. Detailed Model of the Aggregation Event between Two Fractal Clusters. *J. Phys. Chem. B* **2006**, *110*, 6574−6586.
(57) Bothma, J. P.; de Boor, J.; Divakar, U.; Schwenn, P. E.; Meredith, P. Device-Quality Electrically Conducting Melanin Thin Films. *Adv. Mater.* **2008**, *20*, 3539−3542.
(58) Eom, T.; Woo, K.; Cho, W.; Heo, J. E.; Jang, D.; Shin, J. I.; Martin, D. C.; Wie, J. J.; Shim, B. S. Nanoarchitecturing of Natural Melanin Nanospheres by Layer-by-Layer Assembly: Macroscale Anti-inflammatory Conductive Coatings with Optoelectronic Tunability. *Biomacromolecules* **2017**, *18*, 1908−1917.
(59) Salomäki, M.; Tupala, M.; Parviainen, T.; Leiro, J.; Karonen, M.; Lukkari, J. Preparation of Thin Melanin-Type Films by Surface-Controlled Oxidation. *Langmuir* **2016**, *32*, 4103−4112.

https://dx.doi.org/10.1021/acsomega.0c01953
ACS Omega 2020, 5, 25059−25068